

**NANO EXPRESS**

**Open Access**

# Formation mechanisms for the dominant kinks with different angles in InP nanowires

Minghuan Zhang<sup>1,2</sup>, Fengyun Wang<sup>1\*</sup>, Chao Wang<sup>1,2</sup>, Yiqian Wang<sup>1,3\*</sup>, SenPo Yip<sup>4</sup> and Johnny C Ho<sup>4</sup>

## Abstract

The morphologies and microstructures of kinked InP nanowires (NWs) prepared by solid-source chemical vapor deposition method were examined using scanning electron microscopy (SEM) and high-resolution transmission electron microscopy (HRTEM). Statistical analysis and structural characterization reveal that four different kinds of kinks are dominant in the grown InP NWs with a bending angle of approximately 70°, 90°, 110°, and 170°, respectively. The formation mechanisms of these kinks are discussed. Specifically, the existence of kinks with bending angles of approximately 70° and 110° are mainly attributed to the occurrence of stacking faults and nanotwins in the NWs, which could easily form by the glide of {111} planes, while approximately 90° kinks result from the local amorphization of InP NWs. Also, approximately 170° kinks are mainly caused by small-angle boundaries, where the insertion of extra atomic planes could make the NWs slightly bent. In addition, multiple kinks with various angles are also observed. Importantly, all these results are beneficial to understand the formation mechanisms of kinks in compound semiconductor NWs, which could guide the design of nanostructured materials, morphologies, microstructures, and/or enhanced mechanical properties.

**Keywords:** InP nanowires; Kinks; Microstructures; Formation mechanism; HRTEM

**PACS:** 81.07.-b; 81.05.Ea; 81.07.Gf

## Background

Recently, III-V compound semiconductor nanowires (NWs), especially InP NWs, have attracted enormous attention in next-generation electronics, sensors, photonics, and solar cells due to their superior carrier mobilities and as direct and suitable bandgaps for efficient photon coupling [1-6]. In the past decade, most studies have focused on understanding and controlling the morphology and structures of InP NWs, such as tapering, reversible switching of growth direction, twin-plane superlattices, and structural transition [2-4,7-11]. However, to the best of our knowledge, few reports are relevant to the kinked InP NWs, particularly the detailed microstructures related to the bending configuration. Generally, it is believed that the kinks in the NWs would influence their transport properties, electron, and hole collection efficiencies for technological applications [12,13]. In this regard, a detailed study on the formation of these kinks is extremely important,

which could provide valuable information to further design NW materials with different shapes, morphologies, and microstructures, expanding their application domains [14].

In our experiment, kinked InP NWs frequently emerged in the growing process, which possess a crystal structure of face-centered cubic (zinc blende) [6]. In order to understand the growth mechanism of these bending InP NWs, the morphologies and microstructures of different InP NWs were studied utilizing scanning electron microscopy (SEM) and high-resolution transmission electronic microscopy (HRTEM), respectively. Through comprehensive statistical analysis and intensive structural characterization, it is revealed that the dominant bending angles of InP NWs are approximately 70°, 90°, 110°, and 170°. The formation of bending angles of approximately 70° and 110° is mainly attributed to the occurrence of nanotwins and stacking faults (SFs), which could easily form by the glide of {111} planes. However, for approximately 90° bending, local amorphization is believed to be the main cause for this phenomenon while approximately 170° kinks are mostly induced by small-angle boundaries, where the insertion of extra atomic planes could make the NWs slightly bent. In

\* Correspondence: fywang@qdu.edu.cn; yqwang@qdu.edu.cn

<sup>1</sup>The Cultivation Base for State Key Laboratory, Qingdao University, No. 308, Ningxia Road, Qingdao 266071, People's Republic of China

<sup>3</sup>College of Physics Science, Qingdao University, No. 308, Ningxia Road, Qingdao 266071, People's Republic of China

Full list of author information is available at the end of the article

addition, NWs with multiple curves composed of different bending angles are also observed.

## Methods

### Synthesis of InP NWs

InP NWs used in this study were prepared by a solid-source catalytic chemical vapor deposition method in a dual-zone horizontal tube furnace as previously reported [6]. Briefly, the solid source (1 g, InP powder, 99.9999% purity) was placed in a boron nitride crucible and evaporated at the center of the upstream zone, while the growth substrate (0.5 nm Au film deposited on SiO<sub>2</sub>/Si) was placed in the middle of the downstream zone with a tilt angle of approximately 20° and a distance of 10 cm away from the source. Au films with a thickness of 0.5 nm were thermally evaporated under a vacuum of approximately  $1 \times 10^{-6}$  Torr onto the substrates. During the growth of NWs, the substrate was thermally annealed at 800°C for 10 min in a hydrogen environment (99.999% pure H<sub>2</sub>, 100 sccm, 1 Torr) to obtain Au nanoclusters which acted as the catalysts. When the substrate temperature was cooled to the preset growth temperature (460°C), the source was heated to the required source temperature (770°C) for 60 min. After the growth, the source and substrate heater were stopped and cooled down to the room temperature under the flow of H<sub>2</sub> gas.

### Characterization of InP NWs

Philips XL30 SEM (Philips, Amsterdam, Netherlands) was employed to view surface morphologies of the grown InP NWs. Selected-area electron diffraction (SAED), bright field (BF) transmission electron microscopy (TEM), and HRTEM were carried out to determine crystal structure

and to examine microstructures of the grown InP NWs using a JEOL JEM2100F TEM (JEOL Ltd., Tokyo, Japan) operating at 200 kV. The incident electron beam was along the [1 $\bar{1}$ 0] direction. Specimens for HRTEM examinations were prepared by peeling off the InP NWs from the surface of the substrate, ultrasonicated them into anhydrous ethanol for several seconds, and dispersing the finished solution onto a holey-carbon-film-coated copper grid.

## Results and discussion

Figure 1a shows a low-magnification SEM image of InP NWs prepared by 0.5-nm-thick Au catalyst film. It is observed that different kinds of kinks exist in the grown InP NWs. Interestingly, in most cases the bending angles are close to approximately 110° as indicated by white arrows. Magnified SEM image (Figure 1b) exhibits a clear morphology of InP NWs. It is shown that despite there exists some kinks, the overall morphology of grown InP NWs is relatively straight and smooth. As observed from TEM images, InP NWs with kinks can be clearly seen and the diameter of InP NWs is uniform and ranges from 20 to 40 nm. In order to systematically understand the characteristics of the different kinks, initially, a comprehensive statistical analysis was carried out using typical BF TEM images (Figure 1c), which are mainly concentrated in the range of 20 to 30 nm. In this work, the bending angles of more than 180 kinks in different NWs were measured and the statistical result is presented in Figure 1d. It is noted that the angles and frequency of kinks are found independent of the nanowire diameter and four dominant groups of kinks with the bending angles of approximately 70°, 90°, 110°, and 170°

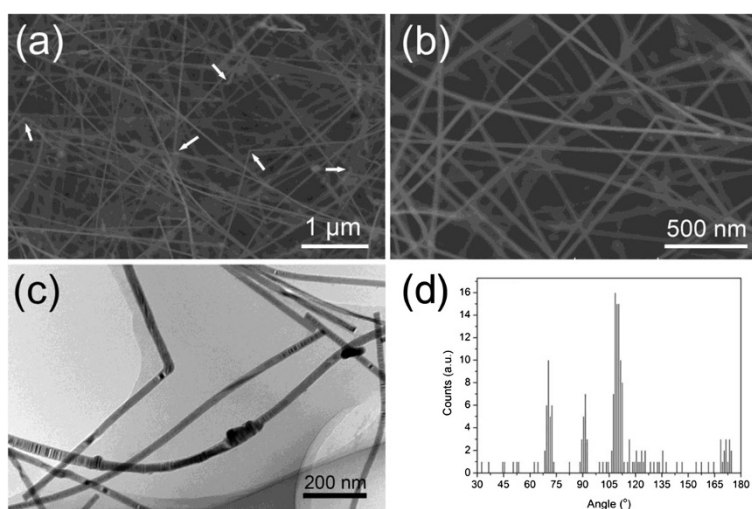


**Figure 1** SEM images depict the morphology of InP NWs along with the statistical graph of kinks. **(a)** Low-magnification SEM image of InP NWs prepared by 0.5-nm-thick Au film. Kinks with different angles are clearly observed. Approximately 110° kinks indicated by white arrows show frequently. **(b)** Magnified SEM image shows clear morphology of InP NWs. **(c)** Typical BF image for angle distribution statistic. **(d)** Kink angle statistics of grown InP NWs observed by TEM images. Four dominant groups of kinks with angles of approximately 70°, 90°, 110°, and 170° are clearly displayed.

are clearly displayed, with the relative percentage of them observed being 17%, 11%, 35%, and 6%, respectively. Except the four dominant groups, the kinked InP NWs with other angles are scarce. Furthermore, the bending angles less than  $30^\circ$  are not observed.

To shed light in exploring the formation mechanism of these kinks with different angles, HRTEM technique was exploited to examine the microstructures of these grown InP NWs. Figure 2 shows the typical BF and HRTEM images of approximately  $110^\circ$  kinks observed in different NWs. It is clear that alternating bright/dark contrast appears in a periodic manner along the axial direction of the wire in BF TEM images (Figure 2a,c,e), which indicates the existence of planar defect structure. The phenomenon is consistent with the previous report that high density of SFs in  $\langle 111 \rangle$ -oriented nanowires commonly form perpendicularly to the growth direction [15]. HRTEM images (Figure 2b,d,f) and corresponding SAED patterns were acquired from the bending areas,

which present explicit illustrations of the microstructures in these kink areas. The SAED patterns (Figure 2a, c insets) show the crystal structure of InP NWs here being face-centered cubic (zinc blende). In Figure 2b, it is obvious that the NWs grows along  $\langle 111 \rangle$  directions and the bending angle is consistent with that between  $(111)$  and  $(\bar{1}\bar{1}1)$  planes, namely, approximately  $110^\circ$ . Since the  $\{111\}$  planes are the faces with lower energy in the face-centered cubic structure, the growth of NWs through  $\{111\}$  planes is energetically favorable. Figure 2b also reveals a stacking fault, almost transecting the entire nanowire in the kink area. We suppose that the transecting SFs in the kinked area would be beneficial to the change of growth direction. In addition, nanotwins and SFs were also observed in the region close to approximately  $110^\circ$  kink as depicted in Figure 2d, which corresponds to the selected area in Figure 2c. As mentioned in the previous report [16], the bending of nanowires typically associated with a significantly large local strain in which SFs are

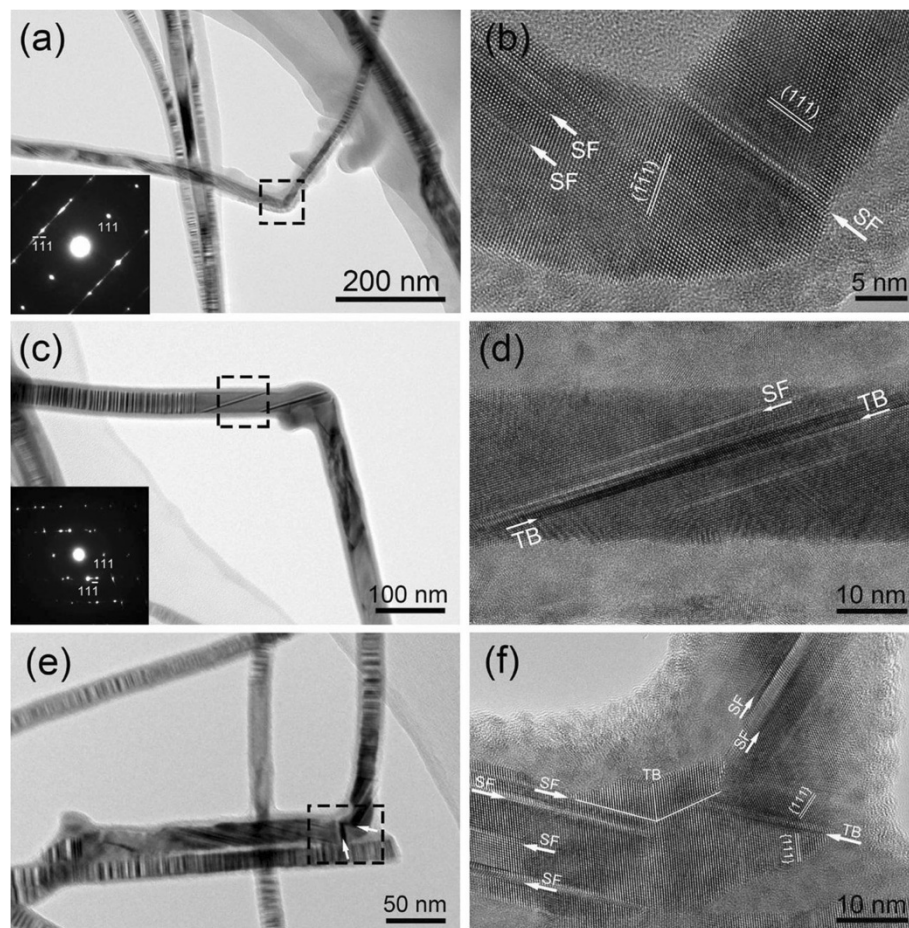


**Figure 2** BF and HRTEM images of approximately  $110^\circ$  kinks in different NWs. (a, c, e) BF images of  $110^\circ$  kinks. Insets in (a) and (c) are SAED patterns corresponding to the selected areas. Clear contrast changes are indicated by white arrows in (e). (b, d, f) are HRTEM images corresponding to the selected areas in (a), (c), and (e) separately. SFs are observed in the kink area in (b). In (d), SFs and twins are shown in the adjacent region to the kink. Large numbers of SFs are observed along the growth direction shown in (f), while twins were observed in the kink area.

induced and resulted to releasing the stress. It is as well noted that an approximately  $110^\circ$  kink consisted of successive curves is observed in Figure 2e. Noticeable contrast variations indicated by white arrows in Figure 2e are supposed to be imaging effects which occur when twin boundary relaxations are present, although it should be pointed out that images with similar appearances could result from astigmatism or misalignment [17]. HRTEM image corresponding to the selected area in Figure 2e is presented in Figure 2f. It is obvious that there is large amount of SFs in the region of approximately  $110^\circ$  kink. In this case, we believe that the larger local strain could be introduced by two successive curves in such narrow space. It is noted that most SFs in the kinked area run nearly parallel to the growth direction. We suppose that in the kinked area, a large amount of stress is introduced such that the  $\{111\}$  planes nearly parallel to the growth direction can easily glide and could facilitate the formation of SFs, which plays an important role in releasing the stress. In addition, nanotwins marked by TB are observed in the bending area. According to the literature, twin-plane formation in zinc blende crystals requires very little energy [18]. The twins

are as expected for bulk zinc blende crystals, which can twin on  $\{111\}$  planes by rotating through  $60^\circ$  about the  $\langle 111 \rangle$  axis [19]. Consequently, in theory, nanotwins could facilitate the NWs to switch from one favorable growth direction to another.

Compared with approximately  $110^\circ$  kinks, the approximately  $70^\circ$  kink bends sharply as shown in Figure 3a. Its corresponding SAED pattern (inset) matches well with cubic zinc blende structure, and the lattice planes are  $\{111\}$  planes. As shown in Figure 3b, the nanotwin appears in the bending area, which is similar to that occurs in approximately  $110^\circ$  kinks. As mentioned above, the formation of nanotwin could be beneficial to the change of growth direction. In addition, it is worth noting that highly dense SFs are also observed in the approximately  $70^\circ$  kink area and nearly parallel to the growth direction. In such a sharp bending, the strain is so severe, which could produce the internal stress larger than that in approximately  $110^\circ$  kink.

On the basis of the above observed results, approximately  $70^\circ$  and  $110^\circ$  kinks are believed to form by the glide of  $\{111\}$  planes, which produces nanotwins and SFs

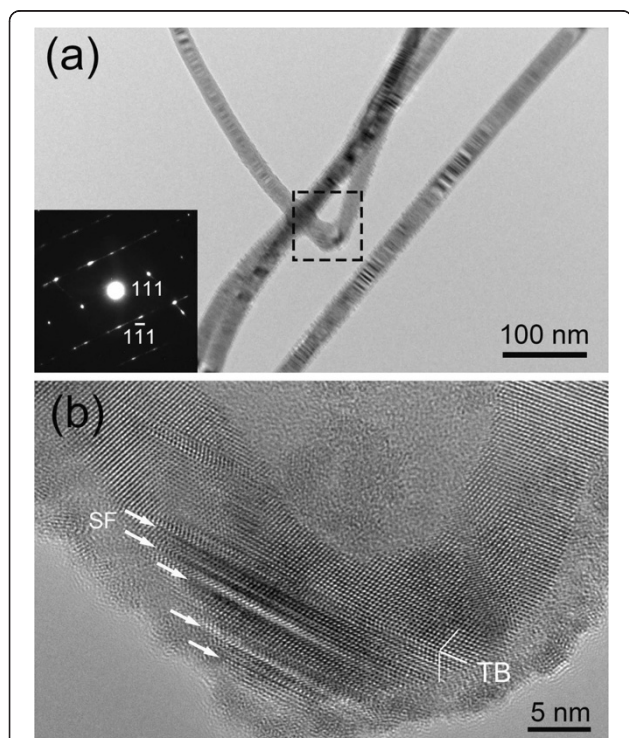


**Figure 3** BF image with corresponding SAED pattern and HRTEM image of approximately  $70^\circ$  kink in InP NWs. (a) BF image of approximately  $70^\circ$  kink in InP NWs. The SAED pattern from the kink area (inset) matches with cubic zinc blende structure. (b) HRTEM image of the selected region in (a). Dense SFs indicated by white arrows emerge in the kink area. The twin indicated by TB appears in the kink area.

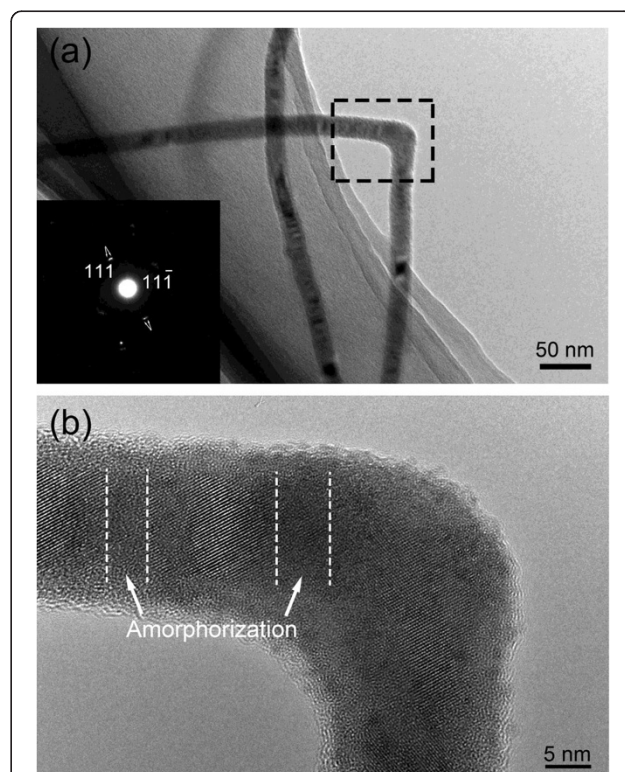
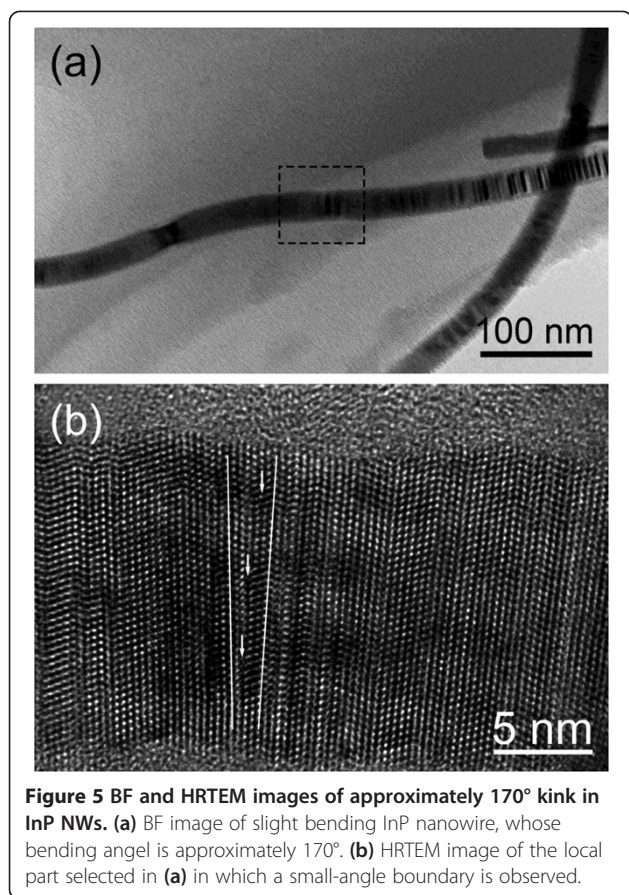


**Figure 4** BF image with corresponding SAED pattern and HRTEM image of approximately  $90^\circ$  kink in InP NWs. (a) BF image of the kink of approximately  $90^\circ$  in InP NWs. The inset is SAED pattern corresponding to the kink in which the diffraction spots indicated by white arrows are split into irregular spots. (b) HRTEM image of the selected area in (a). The observed amorphous regions are pointed by arrows.

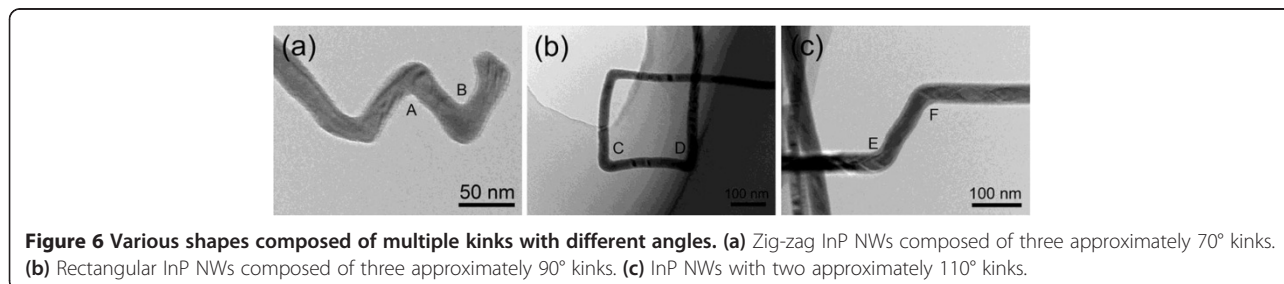


to facilitate the formation of such kinks. It is known that {111} planes are the closest packed planes with the lower interfacial energy in cubic zinc blende structure and the angles between two different {111} planes are 70.5° or 109.5°. Therefore, the change of growth direction is inclined to be <111> and the bending angle is mostly close to 70.5° or 109.5°. However, due to their difference in the bending degree, the densities of SFs in local areas for approximately 70° and 110° kinks are different. When the bending angle is approximately 70°, the curvature is so sharp and supposed to cost larger energy. As a result, the internal stress would be larger than that of approximately 110° kinks, which needs massive and dense SFs to release. In addition, the sharp curvature makes the formation of approximately 70° kinks more difficult,

which can be interpreted by presence of a smaller percentage with approximately 70° kink than that of approximately 110° kink as illustrated in Figure 1d.

In the previous studies, SFs and nanotwins are frequently observed in III-V semiconductor NWs [7,9,20]. Here, the intensive study of microstructures reveals some novel characteristics in the remaining two groups of kinks in InP NWs, i.e., approximately 90° kinks and 170° kinks. As presented in Figure 4a, an approximately 90° kink can be clearly observed. The inset gives its corresponding SAED pattern, in which each diffraction spot indicated by white arrows was split into adjacent irregular spots. It indicates that the crystal orientation makes slight changes in this area. It is evidenced in Figure 4b that the amorphous regions pointed by arrows are firstly observed in the approximately 90° kink, where the crystal orientation is disordered. This result could guide us presenting reasonable explanations for the formation of approximately 90° kinks. In crystallography, it is not easier to form an approximately 90° angle by the glide of {111} planes. Therefore, in order to produce such shape, the change of crystal lattice becomes reasonable. It is known that amorphization could distort the crystal lattice and break the barrier for the transition of morphology in the growing process. As a result, the growth of NWs would become more flexible, which is beneficial to the formation of approximately 90° kinks.

As for the slight bendings, i.e., approximately 170° kinks, careful examinations show that the small-angle boundary exists in the bending area, being rarely observed in III-V semiconductor NWs [16]. As depicted in Figure 5a, the InP NWs are slightly bent in which planar defects could be easily observed. Furthermore, as given in Figure 5b, a small-angle boundary was clearly seen in the selected area of Figure 5a. The extra atomic planes are inserted as indicated by arrows. This result is similar to that observed in Au NWs [21]. In the growing process, the NWs are likely to be affected by the disturbance of growth conditions, such as the gas flow fluctuation. As a result, the atomic arrangement is likely to collapse and tend to reconstruct in order to accommodate the disturbance effect, which causes the formation of small-angle boundary. The inserted extra atomic planes could generate unbalanced internal stress for the



growth of the upper side and lower side of InP NWs shown in Figure 5b. Consequently, the InP NWs show slight bending. In addition, depending on the simulation of Cao et al. [22], the motion of dislocations along the well-defined slip systems can be restricted by twin boundaries (TBs). As observed, there are plenty of TBs in the left and right sides of the small-angle boundary, which would restrict the occurrence and the motion of dislocations. Therefore, the number of kinks with approximately  $170^\circ$  is relatively small.

In addition to individual kinks, multiple kinks are also frequently observed in InP NWs. As shown in Figure 6, different shapes, such as zig-zag and rectangle, are composed of kinks with different angles mentioned above. They are likely to be formed by the change of growth conditions. At the same time, it is observed that the formation of kinks is not related to the substrate tilting during the growth. For the growth substrate without any tilt angle, the InP NWs with kinks were also frequently observed. The occurrence of continuous kinks means that there is a possibility to produce NWs with different shapes in large scale, such as the nanospring produced in ZnO NWs [16]. Our results also call into question how to control the shape and microstructures of NWs by tuning the NW growth conditions in order to satisfy the needs of practical applications.

## Conclusions

In conclusion, four dominant kinds of kinks with an angle of approximately  $70^\circ$ ,  $90^\circ$ ,  $110^\circ$ , and  $170^\circ$  have been observed in InP NWs. The dominant InP crystal structure in this work is zinc blende and the kinks with bending angles of approximately  $70^\circ$  and  $110^\circ$  are mainly attributed to the SFs and nanotwins, which could easily form by the glide of  $\{111\}$  planes. However, the approximately  $90^\circ$  kinks result from the local amorphization of InP NWs while the approximately  $170^\circ$  kinks are mainly caused by small-angle boundaries, where the insertion of extra atomic planes could make the NWs slightly bend. In addition, NWs with multiple kinks in various angles are also observed.

## Abbreviations

BF: Bright field; HRTEM: high-resolution transmission electronic microscopy; NWs: nanowires; SAED: selected-area electron diffraction; SEM: scanning electron microscopy; SFs: stacking faults; TBs: twin boundaries.

## Competing interests

The authors declare that they have no competing interests.

## Authors' contributions

MHZ analyzed the experimental results and drafted the manuscript. FYW performed the SEM observations and revised the manuscript. CW performed the HRTEM observations. YQW proposed the formation mechanism of the kinks in InP NWs and revised the manuscript. SPY and FYW fabricated InP NWs. JCH directed the experiment of fabricating InP NWs. All authors read and approved the final manuscript.

## Acknowledgements

The work is financially supported by National Key Basic Research Development Program of China (grant no. 2012CB722705), the Natural Science Foundation for Outstanding Young Scientists in Shandong Province, China (grant no. JQ201002), the Program for Foreign Cultural and Educational Experts (grant nos. W20123702084, W20133702021), and the Early Career Scheme of the Research Grants Council of Hong Kong SAR, China (grant no. CityU139413). YQW would like to thank the financial support from the Top-notch Innovative Talents Program of Qingdao City and the Taishan Scholar Program of Shandong Province, China.

## Author details

<sup>1</sup>The Cultivation Base for State Key Laboratory, Qingdao University, No. 308, Ningxia Road, Qingdao 266071, People's Republic of China. <sup>2</sup>College of Chemistry and Chemical Engineering, Qingdao University, No. 308, Ningxia Road, Qingdao 266071, People's Republic of China. <sup>3</sup>College of Physics Science, Qingdao University, No. 308, Ningxia Road, Qingdao 266071, People's Republic of China. <sup>4</sup>Department of Physics and Materials Science, City University of Hong Kong, 83 Tat Chee Avenue, Kowloon, Hong Kong.

Received: 24 March 2014 Accepted: 20 April 2014

Published: 5 May 2014

## References

1. Duan X, Huang Y, Cui Y, Wang J, Lieber CM: Indium phosphide nanowires as building blocks for nanoscale electronic and optoelectronic devices. *Nature* 2001, **409**:66–69.
2. Han N, Wang F, Hou JJ, Yip SP, Lin H, Xiu F, Fang M, Yang Z, Shi X, Dong G, Hung TF, Ho JC: Tunable electronic transport properties of metal-cluster-decorated III-V nanowire transistors. *Adv Mater* 2013, **25**:4445–4451.
3. Johansson J, Karlsson LS, Svensson CP, Martensson T, Wacaser BA, Deppert K, Samuelson L, Seifert W: Structural properties of  $\langle 111 \rangle$ -B-oriented III-V nanowires. *Nat Mater* 2006, **5**:574–580.
4. Caroff P, Dick KA, Johansson J, Messing ME, Deppert K, Samuelson L: Controlled polytypic and twin-plane superlattices in III-V nanowires. *Nat Nanotechnol* 2009, **4**:50–55.
5. Han N, Hou JJ, Wang F, Yip S, Yen YT, Yang ZX, Dong G, Hung T, Chueh YL, Ho JC: GaAs nanowires: from manipulation of defect formation to controllable electronic transport properties. *ACS Nano* 2013, **7**:9138–9146.
6. Hui AT, Wang F, Han N, Yip S, Xiu F, Hou JJ, Yen YT, Hung T, Chueh YL, Ho JC: High-performance indium phosphide nanowires synthesized on amorphous substrates: from formation mechanism to optical and electrical transport measurements. *J Mater Chem* 2012, **22**:10704.
7. Ikejiri K, Kitauchi Y, Tomioka K, Motohisa J, Fukui T: Zinc blende and wurtzite crystal phase mixing and transition in indium phosphide nanowires. *Nano Lett* 2011, **11**:4314–4318.
8. Wang J, Plissard SR, Verheijen MA, Feiner LF, Cavalli A, Bakkers EP: Reversible switching of InP nanowire growth direction by catalyst engineering. *Nano Lett* 2013, **13**:3802–3806.
9. Dick KA, Caroff P, Bolinsson J, Messing ME, Johansson J, Deppert K, Wallenberg LR, Samuelson L: Control of III-V nanowire crystal structure by growth parameter tuning. *Semicond Sci Tech* 2010, **25**:024009.
10. Glas F, Harmand JC, Patriarche G: Why does wurtzite form in nanowires of III-V zinc blende semiconductors? *Phys Rev Lett* 2007, **99**:146101.
11. Kitauchi Y, Kobayashi Y, Tomioka K, Hara S, Hiruma K, Fukui T, Motohisa J: Structural transition in indium phosphide nanowires. *Nano Lett* 2010, **10**:1699–1703.
12. Hou JJ, Han N, Wang F, Xiu F, Yip S, Hui AT, Hung T, Ho JC: Synthesis and characterizations of ternary InGaAs nanowires by a two-step growth method for high-performance electronic devices. *ACS Nano* 2012, **6**:3624–3630.
13. Han N, Wang F, Hui AT, Hou JJ, Shan GC, Fei X, Hung TF, Ho JC: Facile synthesis and growth mechanism of Ni-catalyzed GaAs nanowires on non-crystalline substrates. *Nanotechnology* 2011, **22**:285607.
14. Tian B, Xie P, Kempa TJ, Bell DC, Lieber CM: Single-crystalline kinked semiconductor nanowire superstructures. *Nat Nanotechnol* 2009, **4**:824–829.
15. Krishnamachari U, Borgstrom M, Ohlsson BJ, Panev N, Samuelson L, Seifert W, Larsson MW, Wallenberg LR: Defect-free InP nanowires grown in  $[001]$  direction on InP (001). *Appl Phys Lett* 2004, **85**:2077.
16. Wang X, Ding Y, Summers CJ, Wang ZL: Large-scale synthesis of six-nanometer-wide ZnO nanobelts. *J Phys Chem B* 2004, **108**:8773–8777.

17. Marks L, Smith DJ: HREM and STEM of defects in multiply-twinned particles. *J Microsc* 1983, **130**:249–261.
18. Hurlle D, Rudolph P: A brief history of defect formation, segregation, faceting, and twinning in melt-grown semiconductors. *J Cryst Growth* 2004, **264**:550–564.
19. Korgel BA: Semiconductor nanowires: twins cause kinks. *Nat Mater* 2006, **5**:521–522.
20. Algra RE, Verheijen MA, Borgstrom MT, Feiner LF, Immink G, Van Enckevort WJ, Vlieg E, Bakkers EP: Twinning superlattices in indium phosphide nanowires. *Nature* 2008, **456**:369–372.
21. Wang C, Wei Y, Jiang H, Sun S: Bending nanowire growth in solution by mechanical disturbance. *Nano Lett* 2010, **10**:2121–2125.
22. Cao AJ, Wei YG, Mao SX: Deformation mechanisms of face-centered-cubic metal nanowires with twin boundaries. *Appl Phys Lett* 2007, **90**:151909.

doi:10.1186/1556-276X-9-211

**Cite this article as:** Zhang et al.: Formation mechanisms for the dominant kinks with different angles in InP nanowires. *Nanoscale Research Letters* 2014 **9**:211.

**Submit your manuscript to a SpringerOpen<sup>®</sup> journal and benefit from:**

- ▶ Convenient online submission
- ▶ Rigorous peer review
- ▶ Immediate publication on acceptance
- ▶ Open access: articles freely available online
- ▶ High visibility within the field
- ▶ Retaining the copyright to your article

---

Submit your next manuscript at ▶ [springeropen.com](http://springeropen.com)

---